Optimizing the Emission Oscillator Strength Based on the Molecular Length Manipulation Strategy

Saba Razaq Salman[1], Oday A. Al-Owaedi[2]
[1], [2]Department of Laser Physics, College of Science for Women, University of Babylon, Hilla 51001, Iraq
Email: pure.saba.rasaq@uobabylon.edu.iq
Email: oday.alowaedi@uobabylon.edu.iq

Abstract
The thiophene/phenylene co-oligomers (TPCOs) is characterised by the molecular layered structure,this structure being very often observed for crystals of ''direction-defined'' long molecules with a large aspect ratio .The electronic, electric, thermoelectric and spectral properties for a series of molecule with different molecular length (P3T,P5T,P7T,P9T,P11T)are studied to explore the fundamental transport mechanisms for electrons crossing through single molecules.we probed emission streangth osillator ,electrical conductance and Seebeck coefficient i-V characterastic for Au| organic molecule|Au configurations using the density functional theory Our results confirmed that increasing the molecular length leads to improved optical, electronic and thermoelectric properties, and thus the possibility of using these particles as effective laser media.
Keywords: The thiophene/phenylene co-oligomers, Emission Oscillator Strength, Electrical conductance

1. Introduction

Over the years, great efforts have been devoted to the development of organic solid-state lasers (OSSL) due to the easy and economic fabrication, covering a wide-range lasing wavelength from near infrared to ultraviolet [1-6]. To date, optically pumped OSSL have been maturely developed, with the achievement of remarkably low laser and/or amplified spontaneous emission (ASE) thresholds and quasi-continuous wave operation [7,8]. The ultimate goal in the field of OSSL is, however, to realize electrically pumped lasing so as to truly enable the creation of low-cost, portable, and flexible solid OSSL devices. Compared to optically pumped OSSL, lasing under electrical pumping is much more challenging because of the following factors. First, triplet exciton tends to accumulate under electrical pumping based on spin statistics [9], that is, three quarters of excitons formed under current injection are triplets, which usually have a long decay time [8]. Second, under electrical pumping, multiple annihilation and absorption losses will be induced by polarons, excitons, and other species that are not involved in optical pumping [8,6]. Recently, there are encouraging progresses reporting promising indications of current injection OSSL [10], which opened up the opportunities in realizing compact and low cost electrically driven organic laser devices. Notwithstanding the advancements achieved in previous studies [10], obstacles still remain for organic laser gain media to observe light amplification under electrical pumping. Therefore, it is of significant importance to carry out theoretical evaluation and predict potentially good electrical pumping candidates, which require a large, stimulated emission cross section [9,10].

2. Results and Discussion

The crystal structure of the thiophene/phenylene co-oligomers (TPCOs) is characterised by the molecular layered structure, this structure being very often observed for crystals of ''direction-defined'' long molecules with a large aspect ratio [11]. As far as the straight-chain molecules like oligophenylenes are concerned, the layered structure can be seen for the compounds of two aromatic rings or more . In their crystals, the molecules tend to be disposed with the molecular long axes tilting with respect to the bottom crystal plane [11,12,13]. The tilting can be measured by an angle between the molecular long axis and the normal to The bottom crystal plane [14,15]. In the case of the straight-chain molecules the said angle is around 10–20° [11]. The tilting angles, however, are generally small with the non-straight molecules typified by the TPCOs [16-17]. Here the molecular long axis is defined as a line connecting the terminal carbon atoms of the molecule. In the case of phenyl (thiophene) terminals, the relevant carbon atoms are located at the p-position on phenyls (α-position of thiophenes) [16-18]. Figure 1 shows optimized molecules under study in this paper The structural aspects of these molecules are distinguished by various molecular lengths, since the shortest molecule (P3T) has a molecule length of 2.089 nm, while the longest one (P11T) posses 5.271 nm. All structural aspects are

doi.org/10.31838/hiv23.02.57 Received: 09.10.22, Revised: 05.11.22, Accepted: 20.12.22

shown in Table 1.

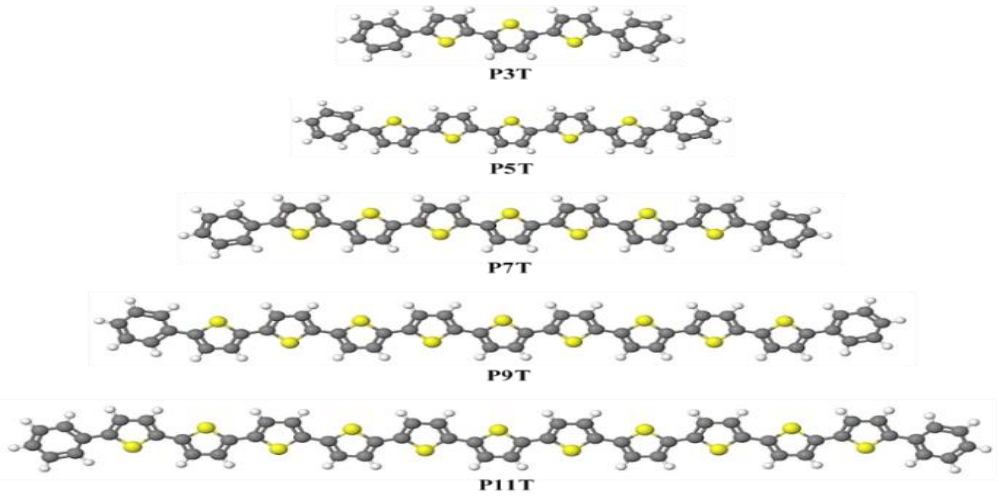

Figure 1. The optimized single molecules.

Table 1. The structural aspect of all molecules. L (H…H), is the molecule length, D (Au…Au), is the molecular length. X is the bond length (Au…C). Z (D – 0.25), is the theoretical electrodes separation. C–C is the carbon-carbon single bond. C=C is the carbon-carbon double bond. C–S is the carbon-sulfur single bond.

Molecule	L (nm)	D (nm)	X (nm)	Z (nm)	C–C (nm)	C=C (nm)	C–S (nm)
P3T	2.089	2.376	0.245	2.126	0.149	0.139	0.168
P5T	2.866	3.155	0.245	2.905	0.149	0.139	0.168
P7T	3.653	3.940	0.245	3.69	0.149	0.139	0.168
P9T	4.442	4.720	0.245	4.47	0.149	0.139	0.168
P11T	5.271	5.561	0.245	5.311	0.149	0.139	0.168

To provide further insight, and to better evaluate the properties and behaviour of these molecular junctions, calculations using a combination of DFT and a nonequilibrium green's function formalism were also carried out. Eight layers of (111)-oriented bulk gold with each layer consisting of 6×6 atoms and a layer spacing of 0.235 nm were used to create the molecular junctions, as shown in Figure 2. The optimized molecular junction geometries conform well to a description of the phynel-gold contacted compounds forming an angle of 160° contact between the carbon anchor atom and the under coordinated gold atoms of the gold electrodes. As expected, Figure 2, and Table 1 show that the phynel contacted compounds are oriented normal to the idealized pyramidal gold electrode surface within the molecular junction. Also, the molecular length of structures increases with increasing of sulfur atoms from 3 sulfur atoms for the shortest molecule to 11 atom for the longest molecule.

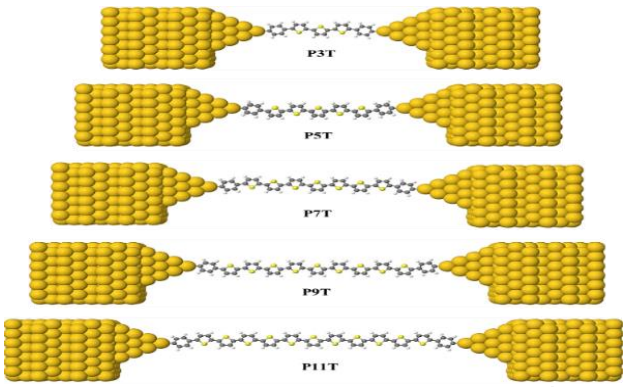

Figure 2. The optimized molecular junction of all structures.

Figure 3. presents the absorption and emission results for all molecules under study. Initially, it can be noticed that the absorption intensity of molecules have increased with increasing of the molecule length from 70000 (a.u.) to 180000 (a.u.). In fact, figure 3. illustrates that P3T molecule has the smallest emission oscillator strength (fem) (1.6), while the highest value of fem is intrudesed via P11T molecule as shown in Figure 4 and Table 2. Since, the calculated emission cross section σem of a laser transition is consider an important parameter in a laser gain medium. It can affect laser performance in terms of threshold energy, output energy, maximum gain, etc.σem is directly proportional to the emission oscillator strength fem via [19]:

$$\sigma_{em}(v) = \frac{e^2}{4\varepsilon_0 m_e c_0 n_F} g(v) f_{em}$$

where e is the electron charge, ε0 is the vacuum permittivity, me is the mass of electron, c0 is the speed of light, nF is the refractive index of the gain material, ν is the frequency of the corresponding emission, and $g(v)$ is the normalized line shape function with $\int g(v)\, dv = 1$. According to the aforementioned facts, all molecules have a high value of fem, which directly leads to high σem, and therefore any of these materials is possible to be a good optical gain medium in practice. In addition, these results predicate a fact that the molecules with short molecule length properties (see Figure 4 and Table 2), possess a lower fluorescence, and hence they are not suitable for laser gain media, which is consistent with references [20,21]. On the other hand, molecules with a long molecule length have a good emission oscillator strength (fem), since they

owned fem > 2, and that means those structures are promising candidates for laser gain medium. Furthermore, most of molecules have produced the maximum emission at wavelengths ranging from 558 to 688 nm, which is in the visible region. These results bring us to an important outcome that those molecules could be powerful for the optoelectronic applications such as light emitting diodes.

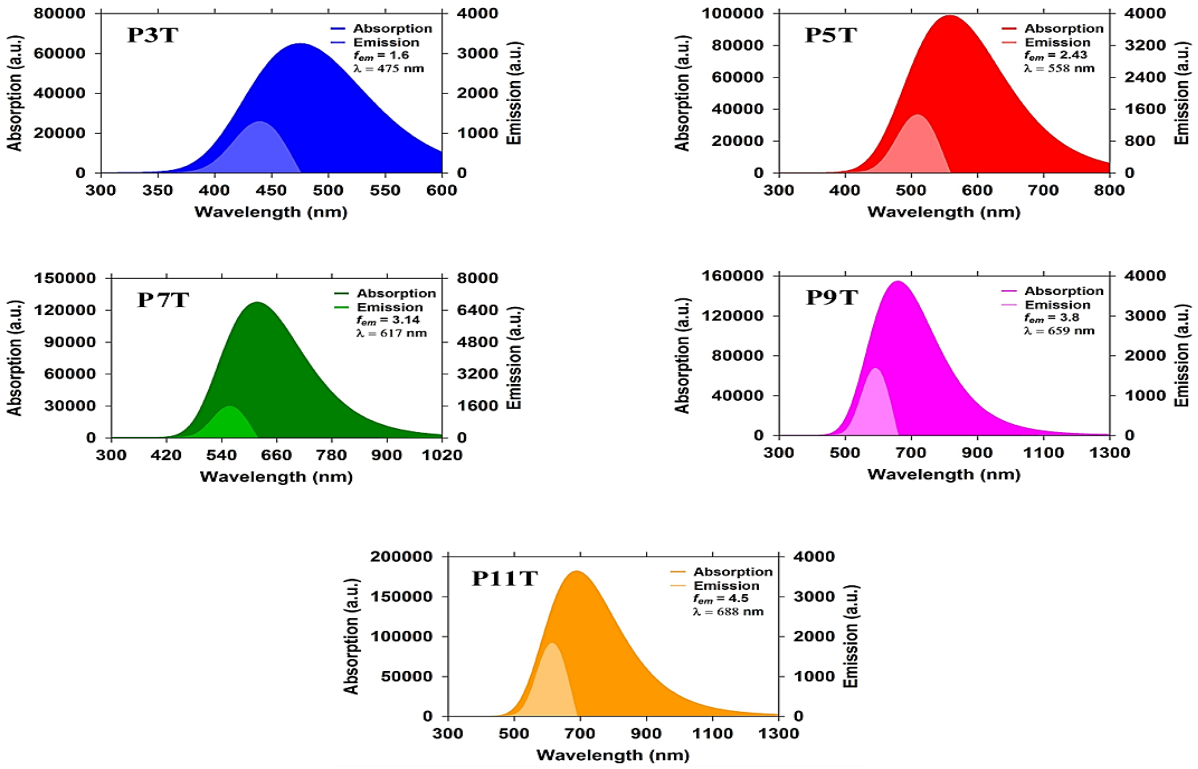

Figure 3. Represents the absorption, emission and emission oscillator strength of all molecules.

Table2. Emission strength oscillator (fem). Maximum wavelength (λMax).. HOMOs and LUMOs energies. HOMO-LUMO energy gaps.

Molecule	fem	λMax (nm)	HOMO (eV)	LUMO (eV)	H-L Gap (eV)
P3T	1.6	475	1.4	1.0	2.14
P5T	2.43	558	1.2	0.9	2.1
P7T	3.14	617	1.13	0.8	1.93
P9T	3.8	659	1.1	0.8	1.90
P11T	4.5	688	0.87	0.56	1.43

The electronic structure calculations of any system are an important tool to explore and understand the different properties of molecules. Therefore, the charge distribution, energies, and molecular orbitals (HOMOs and LUMOs), for all molecules have been calculated using the Gaussian package [20-22], as shown in Figure.4.

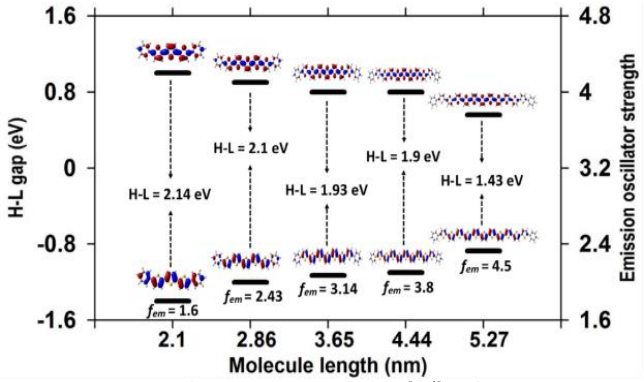

Figure 4. Iso-surfaces (±0.02 (e/bohr^3)$^{1/2}$) of the HOMOs and LUMOs, and emission oscillator strength for all molecules.

First of all, these results show that the value of HOMO-LUMO gap has been varied from 2.14 eV for P3T to 1.9 eV for P9T. Then, it dramatically shrinked from to 1.43 eV for P11T. These results can be ascribed to the influence of the quantum size effect, which its influence appears due to changing the molecule length from 2.089 nm for P3T to 5.271 nm for P11T. An important point that can be observed from Figure 4, that the HOMOs and LUMOs of the first two molecules P3T and P5T are more character over all the backbone of these molecules. While the rest of structures showed weight less of HOMOs and LUMOs, and that could explain in terms of long tunnelling distance that have been propagated via electrones. These results may aid to put a suitable interpretation of the emission oscillator strength results shown in Figure 4. Since the lowest value of fem (1.6) is introduced by P3T molecule, which has the shortest molecule length (2.089 nm), as shown in Table 1 and Figure1, and the biggest HOMO-LUMO gap (2.14 eV). Then, the emission oscillator strength increased dramatically with increasing of molecule

length to reach the highest value (4.5 nm) for P11T molecule, which possess the longest molecule length (5.271 nm), and the lowest HOMO-LUMO gap (1.43 eV).

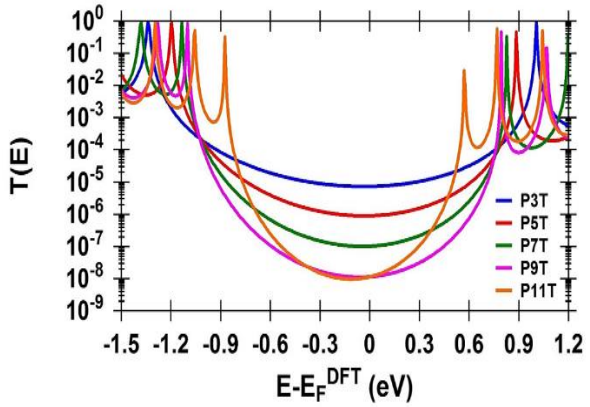

Figure 5. Represents the transmission coefficient as a function of the electron's energy of all molecular junctions.

These results can be interpreted in terms of the combine of electrons path and quantum size effects, since the increasing of thiophene unites increased the length of electrons path, which increased the tunnelling distance and that resulted to decrease the transmission coefficient value. In contrast, the width of the HOMO-LUMO gap becomes narrow with increasing of the molecular length, which ascribed to the impact of the quantum size role. Depending on this, it can be observed that the shortest molecule P3T (2.089 nm) as shown in Figure 1, exhibits the highest transmission (7.44×10-6) as shown in Figure 4 and the widest HOMO-LUMO gap (2.14 eV), while the longest molecule P11T (5.271 nm) offers the lowest transmission (1.15×10-8) and narrowest gap (1.43 eV). In general, the transmission coefficient value of all molecules is high, and that can understand in terms of the quantum interference is a constructive interference and there is not a destructive interference signature within the gap. The order of the transmission is T(E)P3T > T(E)P5T > T(E)P7T > T(E)P9T > T(E)P11T. In the same way, the order of HOMO-LUMO gap is H-L gapP3T > H-L gapP5T > H-L gapP7T > H-L gapP9T > H-L gapP11T. These results support the previous outcomes and provide a rubest evidence that increasing the molecular length led on the one hand to reduce the HOMO-LUMO gap, which effectively contributed to creating the radiative recombination mechanism of charge carriers, which in turn led to a significant increase in the emission oscillator strength, and a sharp lowering of the electronic transmission coefficient.

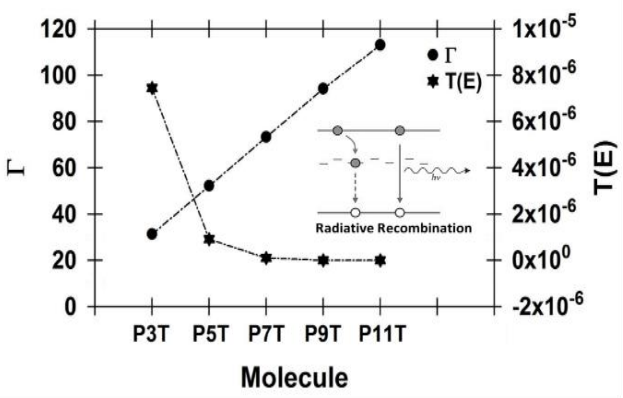

Figure 7. The transferred electrons from molecule (Γ), and the electronic transmission coefficient of all molecules.

Figure 7 shows a very important result, especially for this kind of molecules, as it is known that increasing the number of tranfered electrons leads to an increase in the transmission coefficient, but the exact opposite is provided by the results presented in Figure 7. Notably, the molecule T3P, that possess the lowest Γ value, grants the highest transmission coefficient. The contrary is true for the T11P molecule, which has the highest value of Γ and the lowest value for the transition coefficient. These transport electrons of molecules T5P, T7P, T9P and T11P could be lost only in one way, which is the recombination process. Therefore, these results confirm and support the previously presented results, which predicted that this type of structures could be an effective organic current-injected laser device and light-emitting transistors (LETs), because the recombination processes of the charge carriers in this type of molecules occur frequently and very effectively as shown in the inset of the Figure 7. These processes, in turn, lead to a significant increase emission oscillator strength, as shown in Figure 3.

Table 3. e_M is the number of electons on molecule in a gas phase. e_J is the number of electons on molecule in a junction. Γ is the transferred electrons. T(E) is the transmission coefficient.

Molecule	eM	eJ	Γ	T(E)
P3T	48	16.64	31.36	7.44×10-6
P5T	80	27.70	52.29	9.09×10-7
P7T	112	38.77	73.22	1.03×10-7
P9T	144	49.84	94.15	1.20×10-8
P11T	176	62.00	113	1.15×10-8

Now, it is interesting to consider what would happen with the thermoelectric properties of a single molecule junction as a function of the molecular length. Here this study will show that the thermoelectric properties, thermopower (S), electrical conductance (G/G_0) and current-voltage (I-V), characterized by the electronic figure of merit (ZT_e), can be tuned as a function of the theoretical electrode separation, in a single PT molecule junction (Au/TP/Au). This study also propose a strategy to obtain the maximum ZT of molecular junctions in general.

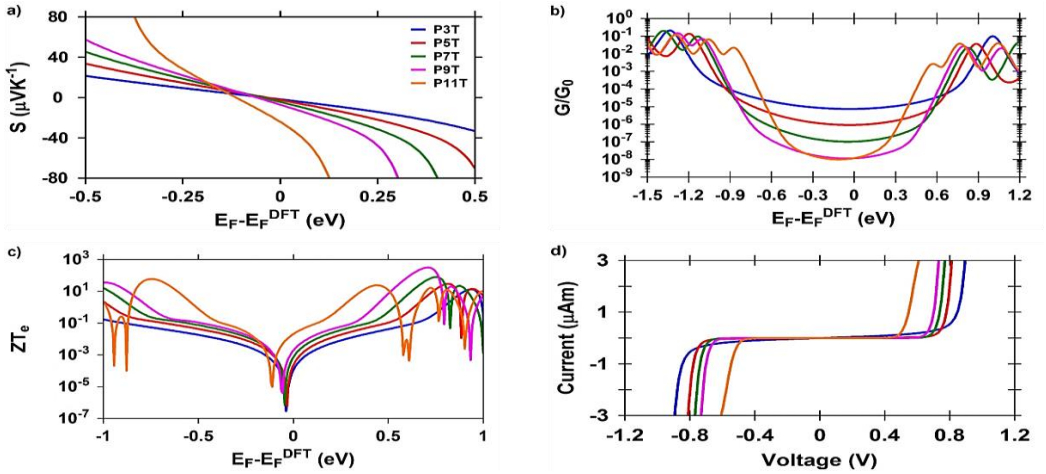

Figure 4.9. a) Thermopower (S) as a function of Fermi energy; b) Electrical conductance (G/G0) as a function of Fermi energy; c) Electronic figure of merit (ZTe) as a function of Fermi energy; d) Current-Voltage characteristics.

The computed values of the thermopower were nagative and ranging between -1.55 μVK-1 for P3T to -23.42 μVK-1 for P11T as shown in figure 9a and Table.4. These results demonstrate an important role of the occupied molecular orbitals in determine the electrons transport mechanism which is a LUMO-dominated, and so the value and sign of the thermopower for all molecules. The midgap mechanism (see Figure 9b) points out that the position of Fermi energy is also a significant parameter because a small change in it could leads to different results for the conductance and thermopower. Figure 9c shows the results of the electronic figure of merit, which is a quantity used to characterize the performance of a device, system or method, relative to its alternatives. Interestingly, the molecule P3T exhibits the lowest figure of merit (9.66×10-5), while the highest value (1.93×10-2) has been shown via molecule P11T. These results prove that the calculated single-molecule conductance value (see Figure 9c), at the most probable Fermi energy is the crucial parameter in determining the value of the figure of merit, even if the thermopower value was high. Undoubtedly, the outcomes of conductance (G), thermopower (S) and electronic figure of merit (ZTe), which illustrated in figures 9abc respectively, indicate to an existence of a relation between these parameters. Since the high G results in a low S, which in turn leads to low ZTe.

Table 4. Thermopower (S). Electrical conductance (G/G_0). Electronic figure of merit (ZT_e). Threshold voltage (V_{th}).

Molecule	S (μVK-1)	G/G0	ZTe	Vth (V)
P3T	-1.55	0.74×10-5	9.66×10-5	0.8
P5T	-2.19	0.92×10-6	1.91×10-4	0.75
P7T	-4.04	0.1×10-6	6.38×10-4	0.7
P9T	-6.66	0.12×10-7	1.71×10-3	0.65
P11T	-23.42	0.1×10-7	1.93×10-2	0.5

3. Conclusions

We have described various features of the thiophene/phenylene co-oligomers (TPCO) materials. It includes the characteristics of the TPCO structures and their relevance to the structure/property relationship.

In relation to the important future application, we dealt with several features associated with the laser oscillation from the organic semiconductors, such as the emission oscillator strength, HOMO-LUMO gap, charges distribution and orbitals, as well as the transmission and seeback coefficients. It could be concluded that molecular length manipulation strategy is an effective method to control and enhance the properties of TPCO-based devices and their applications. Since, the increasing of molecule length enhances noticeably some of spectral, optical and thermoelectric (fem, H-L gap and S) properties, and on other hand it lowers some of electronic (T(E)) properties. We have stressed that the TPCO structures are exceptionally good for light emitting diode and thermoelectric applications. Their structures produce the effective optical quantum confinement and lasing characteristics within the structure, and thus may be an excellent candidate for the laser media. In addition, the TPCO materials are expected to become important to a solar cell development. The TPCOs may play a pivotal role in the field of organic semiconductor materials and their optoelectronic device applications.

References

[1] D. Fichou, S. Delysse, and Nunzi, J.-M. First evidence of stimulated emission from a monolithic organic single crystal: α-Octithiophene. Adv. Mater.

9, 1997 . p. 1178–1181. https://ur.booksc.me/book/271283/c52840.
[2] Samuel, I. D. W. and Turnbull, G. A. Organic semiconductor lasers. Chem. Rev. 107. 2007. p.1272–1295. https://doi.org/10.1021/cr050152i
[3] S. Chénais, and S. Forget, Recent advances in solid-state organic lasers. Polym. Int. 61, 2012. p . 390–406.https://doi.org/10.1002/pi.3173
[4] Cui, Q. H., Zhao, Y. S. and Yao, J. Controlled synthesis of organic nanophotonic materials with specific structures and compositions. Adv. Mater. 26, 2014. p. 6852–6870 . https://doi.org/10.1002/adma.201305913
[5] Kuehne, A. J. C. and Gather, M. C. Organic lasers: recent developments onmaterials, device geometries, and fabrication techniques. Chem. Rev. 116, 2016. p .12823–12864.DOI: 10.1021/acs.chemrev.6b00172
[6] J. Gierschner, S. Varghese, and Park, S. Y. Organic single crystal lasers: amaterials view. Adv. Opt. Mater. 4, 2016. p.348–364.https://doi.org/10.1002/adom.201500531
[7] H. Nakanotani, et al. Extremely low-threshold amplified spontaneous emission of 9,9′-spirobifluorene derivatives and electroluminescence from field-effect transistor structure. Adv. Funct. Mater. 17, 2007. p. 2328–2335 https://doi.org/10.1002/adfm.200700069
[8] A. S. D. Sandanayaka, et al. Quasi-continuous-wave organic thin-film distributed feedback laser. Adv. Opt. Mater. 4, 2016. p. 834–839. https://doi.org/10.1002/adom.201600006
[9] Baldo, M. A., O'Brien, D. F., Thompson, M. E. & Forrest, S. R. Excitonic singlet-triplet ratio in a semiconducting organic thin film. Phys. Rev. B 60, 1999. p. 14422–14428 . https://journals.aps.org/prb/abstract/10.1103/PhysRevB.60.14422
[10] Sandanayaka, A. S. D. et al. Indication of current-injection lasing from an organic semiconductor. Appl. Phys. Express 12, 2019. p. 061010 . https://iopscience.iop.org/article/10.7567/1882-0786/ab1b90
[11] K. N. Baker, A. V. Fratini, T. Resch, H. C. Knachel, W. W. Adams, E. P. Socci and B. L. Farmer, Polymer, 1993, 34, 1571–1587. https://cpsm.kpi.ua/polymer/1993/8/1571-1587.pdf
[12] S. Hotta and K. Waragai, J. Mater. Chem., 1991. 1: p. 835–842. https://pubs.rsc.org/En/content/articlelanding/1991/jm/jm9910100835
[13] S. Hotta and K. Waragai, Adv. Mater., 1993. 5: p. 896–908. https://doi.org/10.1002/adma.19930051204
[14] S. Hotta and M. Goto, Adv. Mater., 2002.14: p. 498–501.
[15] S. Hotta, M. Goto, R. Azumi, M. Inoue, M. Ichikawa and Y. Taniguchi, Chem. Mater., 2004. 16: p. 237–241. https://ur.booksc.me/book/29758855/86a681
[16] T. Yamao, Y. Taniguchi, K. Yamamoto, T. Miki, S. Ota, S. Hotta, M. Goto and R. Azumi, Jpn. J. Appl. Phys., 2007.46: p. 7478–7482.
[17] T. Yamao, Y. Nishimoto, K. Terasaki, H. Akagami, T. Katagiri, S. Hotta, M. Goto, R. Azumi, M. Inoue, M. Ichikawa and Y. Taniguchi, Jpn. J. Appl. Phys., 2010. 49: p. 04DK20. https://iopscience.iop.org/article/10.1143/JJAP.49.04DK20/meta
[18] Ou, Q., Peng, Q., & Shuai, Z. .Computational screen-out strategy for electrically pumped organic laser materials. Nature communications, 2020. 11 (1) :p. 1-10 . https://www.nature.com/articles/s41467-020-18144-x
[19] H. Nakanotani, Furukawa, T., Hosokai, T., Hatakeyama, T., & Adachi, C. . Light amplification in molecules exhibiting thermally activated delayed fluorescence. Advanced Optical Materials, 2017. 5 (12). https://doi.org/10.1002/adom.201700051
[20] H. Huang, Yu, Z., Zhou, D., Li, S., Fu, L., Wu, Y. & Fu, H. , Wavelength-Turnable organic microring laser arrays from thermally activated delayed fluorescent emitters", Acs Photonics, 2019. 6 (12) :p. 3208-3214 . https://pubs.acs.org/doi/10.1021/acsphotonics.9b01051
[21] Ye, H., Kim, D. H., Chen, X., Sandanayaka, A. S., Kim, J. U., Zaborova, E. & Adachi, C. .Near-infrared electroluminescence and low threshold amplified spontaneous emission above 800 nm from a thermally activated delayed fluorescent emitter. Chemistry of Materials, 30 (19): p. 6702-6710, 2018. https://doi.org/10.1021/acs.chemmater.8b02247
[22] D. Kim, H. D'aléo, A., Chen, X. K., Sandanayaka, A. D., Yao, D., Zhao, L. & Adachi, C. . High-efficiency electroluminescence and amplified spontaneous emission from a thermally activated delayed fluorescent near-infrared emitter. Nature Photonics. 2018. 12(2): p. 98-104. https://kyushu-u.pure.elsevier.com/en/publications/high-efficiency-electroluminescence-and-amplified-spontaneous-emi